Revision 2

Partition of Al between Phase D and Phase H at high pressure: Results from a simultaneous structure refinement of the two phases coexisting in an unique grain

LUCA BINDI,[1,2*] MASAYUKI NISHI,[3,4] TETSUO IRIFUNE[3,4]

[1] Dipartimento di Scienze della Terra, Università di Firenze, Via La Pira 4, I-50121 Firenze, Italy
[2] CNR - Istituto di Geoscienze e Georisorse, sezione di Firenze, Via La Pira 4, I-50121 Firenze, Italy
[3] Geodynamics Research Center, Ehime University, Matsuyama 790-8577, Japan
[4] Earth-Life Science Institute, Tokyo Institute of Technology, Tokyo 152-8550, Japan

ABSTRACT

The crystal structure of the two dense hydrous magnesium silicates Phase D, $MgSi_2H_2O_6$, and Phase H, $MgSiH_2O_4$, synthesized at 45 GPa and 1000 °C and coexisting in the same micron-sized grain, was investigated by single-crystal X-ray diffraction to study the preferential partition of Al between the two structures. In agreement with the literature, Phase D was found to be trigonal, space group $P\bar{3}1m$, with lattice parameters a = 4.752(2), c = 4.314(2) Å, V = 84.37(6) Å^3 (R_1 = 0.020), and Phase H was found to be orthorhombic, space group *Pnnm*, with lattice parameters a = 4.730(2), b = 4.324(2), c = 2.843(2) Å, V = 58.15(5) Å^3 (R_1 = 0.024). The estimated proportion (vol.%) of the two phases from the refinement is $27(2)_{\mathrm{PhD}} - 73_{\mathrm{PhH}}$. The analysis of the geometric details of the two structures shows that Phase D hosts almost all the Al available, whereas Phase H is nearly identical to pure $MgSiH_2O_4$. Overexposed electron-microprobe X-ray maps of the same grain used for the X-ray diffraction study together with WDS spots on the two phases confirmed the structural results. Thus, our results suggest that when Phase D and Phase H coexist, Al is strongly partitioned into Phase D at the expense of coexisting Phase H. At pressure above ~50 GPa, where Phase D is no longer stable, Phase H is able to incorporate the high aluminum contents present in hydrous peridotitic compositions in the deep lower mantle and be stabilized at the expense of Phase D and magnesium silicate perovskite.

KEYWORDS: Phase D, Phase H, aluminum, dense hydrous magnesium silicates, lower mantle, crystal structure, synthesis

INTRODUCTION

Dense hydrous magnesium silicates (DHMS) play a crucial role in the delivery of a significant amount of water to the lower mantle by the subduction of oceanic slabs thus influencing the structure and dynamics of the deep Earth. Until recently, Phase D, $MgSi_2H_2O_6$, has been considered to be the highest-pressure phase among the DHMS (Frost and Fei 1998; Shieh et al. 1998). However, Tsuchiya (2013) and Nishi et al. (2014) found that at pressures above ~50 GPa, Phase D transforms to a new dense hydrous silicate, $MgSiH_2O_4$, labeled Phase H. The crystal structure of Phase H has been recently investigated by Bindi et al. (2014) by means of single-crystal X-ray diffraction and its stability field, in relation to the hydrous AlOOH component, has been studied in detail by Ohira et al. (2014) and Ohtani et al. (2014). These Authors hypothesized the $MgSiH_2O_4$ – $AlAlH_2O_4$ (Al-Phase H) solid solution as potentially the most important hydrous phase present under deep lower mantle conditions.

The key role of Al in expanding the stability of DHMSs at higher temperatures has been also demonstrated for Phase D independently by Ghosh and Schmidt (2014) and by Pamato et al. (2015). The incorporation of high amounts of Al in the structure of Phase D makes this phase stable at temperatures extending to over 2000 °C at 26 GPa (Pamato et al. 2015), implying that subducted oceanic crust could be a significant long-term water reservoir in the convecting lower mantle.

Both Phase D and Phase H have been proven to host Al replacing Mg in solid solution. However, no structural studies have been carried out on the two phases in coexistence to study the preference of Al for one at high pressure. Electron microprobe studies alone could be affected by large uncertainties in the identification of the phases given the very small size and the close chemical formulae.

Here we report the fortuitous recovery of a single micron-sized grain in a run product synthesized at 45 GPa and 1000 °C exhibiting an intergrowth of Phase D and Phase H. This grain gave us the chance to study the partition of Al in the two phases by simultaneous structure refinements of the two phases.

EXPERIMENTAL

Synthesis

Synthesis experiments were conducted using a 1,500-t multi-anvil apparatus (MADONNA-II) at Ehime University (Matsuyama, Japan). We used sintered diamond anvils with a truncated edge length of 1.5 mm as the second-stage anvils. The sample was loaded into a gold capsule. The sample assembly was composed of sintered (Mg,Cr)O and MgO pressure media, with a cylindrical $LaCrO_3$ heater, and a molybdenum electrode. Temperature was monitored by a $W_{97}Re_3$-$W_{75}Re_{25}$ thermocouple. The pressure media and the heater were dried at 1000 °C for 3 hours before assembling the high-pressure cell. Details of the sample assembly are shown in the supplementary information of Nishi et al. (2014). The experiment was performed in the $Mg(OH)_2$-SiO_2-Al_2O_3 system with Mg:Si:Al=1:1.5:0.5 molar ratios. The sample was compressed to 45 GPa at room temperature. Then the temperature was increased to 1000 °C and held constant for 6 h. Phase H prevailed in the run product, being accompanied by minor proportions of Phase D (Fig. 1).

Data collection and crystal-structure refinement

A small crystal (28 × 34 × 52 μm), hand-picked under a reflected light microscope from the run product (Fig. 1), was examined with an Oxford Diffraction Xcalibur 3 diffractometer (X-ray Mo*K*α radiation, $\lambda = 0.71073$ Å) fitted with a Sapphire 2 CCD detector (see Table 1 for details). The crystal was found to be composed of Phase H and Phase D in a proportion (vol.%) roughly estimable to be 73(2)/27, respectively**.** The lattice parameters for the two phases are: $a = 4.730(2)$, $b = 4.324(2)$, $c = 2.843(2)$ Å, $V = 58.15(5)$ Å^3, and $a = 4.752(2)$, $c = 4.314(2)$ Å, $V = 84.37(6)$ Å^3, respectively. The crystal did not show any sign of deterioration under the X-ray beam. Intensity integration and standard Lorentz-polarization corrections were done with the *CrysAlis* RED (Oxford Diffraction 2006) software package. The program ABSPACK of the *CrysAlis* RED package (Oxford Diffraction 2006) was used for the absorption correction. Particular care was devoted to the data collection and reduction of reflections of the two phases given the close geometric relationships between $(001)_{PhH}$ and $(2\bar{1}0)_{PhD}$. The number of extracted, independent reflections was sufficient to identify the correct space group and begin the structure refinement for both phases, which was carried out using the program SHELXL-97 (Sheldrick 2008), starting from the atomic coordinates given by Bindi et al. (2014) for Phase H (space group *Pnnm*) and by Yang et al. (1997) for Phase D (space group $P\bar{3}1m$). Site-scattering values for the two phases were refined using scattering curves for neutral species (Ibers and Hamilton 1974) as follows: Si vs. at the metal sites and O vs. at the anion sites. The O sites were found to be fully occupied, and the occupancy factors were then fixed to 1.00. An isotropic model for both the phases led to $R_1 = 0.024$ for 37 observed reflections $[F_o > 4\sigma(F_o)]$ and $R_1 = 0.020$ for 35 observed reflections $[F_o > 4\sigma(F_o)]$, for Phase H and Phase D, respectively. No hydrogen atoms were located in the difference Fourier maps (ΔF) for the two phases. Fractional atomic coordinates, atomic displacement parameters, bond distances, and geometric parameters for the two phases are shown in Table 2. Table 3[1] lists the observed and calculated structure factors.

Chemical composition

Given the fact that only one crystal with coexisting Phase H and Phase D was available, it was considered too risky to embed and polish it. For this reason, the crystal was placed on a graphite disk on a stub. *K*α X-ray intensity maps of Al, Mg, and Si (Fig. 2) were obtained using a JEOL JXA-8600 electron microprobe operating at an accelerating voltage of 15 kV and a beam current of 300 nA. Beam current variations during map acquisition were ≤ 4 nA. Acquisition times of 180 ms were used. Maps only show X-ray intensity (i.e., neither calibrations nor background corrections were applied).

WDS spots on the two phases were collected at 15 kV accelerating voltage and 20 nA beam current (and a 1 μm beam diameter), with 30 s as counting times. Matrix correction was performed using the Bence and Albee (1968) program modified by Albee and Ray (1970). The standards used were forsterite (Mg) and albite (Al, Si). The two phases were found to be homogeneous within the analytical uncertainty. The average chemical composition is (wt%), SiO_2 47.0(4); MgO 34.0(2); Al_2O_3 3.0(2); total 84.0(2) (four analyses on different spots) corresponding, on the basis of Σ(Si+Mg+Al) = 2, to $Mg_{1.00(3)}[Si_{0.93(5)}Al_{0.07}]O_4H_2$ (H_2O calculated by difference) for Phase H, and SiO_2 50.50(48); MgO 22.58(32); Al_2O_3 14.27(28); total 87.35(40) (three analyses on different spots) corresponding, on the basis of Σ(Si+Mg+Al) = 3, to $Mg_{1.00(6)}[Si_{1.50(7)}Al_{0.50}]O_6H_2$ (H_2O calculated by difference), for Phase D.

RESULTS AND DISCUSSION

Crystal-chemical features of coexisting Phase H and Phase D

The structures of Phase H and Phase D were found to be nearly identical to those reported by Bindi et al. (2014) and Yang et al. (1997). The electron density refined at the metal sites for both the phases is in excellent agreement with the electron microprobe data. In detail, the mean electron number at the octahedral site for Phase H is 13.02(8), well matching the site population obtained at the microprobe ($Mg_{0.500}Si_{0.465}Al_{0.035}$; e^- = 12.97). In Phase D, the largest octahedron was considered to be filled by Mg only (e^- = 12.03), whereas the mean electron number at the other octahedral site is 13.65(7), in good agreement with the site population obtained at the microprobe ($Si_{0.75}Al_{0.25}$; e^- = 13.75). Such a distribution reflects

---

[1] For a copy of Table 3, document item ……., contact the Business Office of the Mineralogical Society of America.

well on the bond distances observed (Table 2). The mean octahedral metal-oxygen distance of 1.958 Å for Phase H is in good agreement with the calculated value for $^{VI}[Mg\text{-}O]_{0.50}$ + $^{VI}[Si\text{-}O]_{0.465}$ + $^{VI}[Al\text{-}O]_{0.035}$ of 1.95 Å (taking into account the ionic radii; Shannon 1976) and nearly identical to that observed in pure $MgSiO_4H_2$ (1.957 Å; Bindi et al. 2014). The bond distance observed at the Mg-site for Phase D of 2.055 Å is slightly shorter than that observed by Yang et al. (1997) for pure $MgSi_2O_6H_2$ (i.e., 2.105 Å), whereas the (Si,Al)-O bond of 1.821 Å is longer than that of pure Si-O (1.805 Å; Yang et al. 1997) because of the presence of Al replacing Si at the site.

We did not observe an increase of the unit-cell volume in Al-bearing Phase D with respect to pure $MgSi_2O_6H_2$. A similar behavior was also noticed by Boffa Ballaran et al. (2010) for super-aluminous Phase D and by Komatsu et al. (2011) for Al-bearing Phase H. These authors observed that the Tschermak $Si^{4+} + Mg^{2+} \leftrightarrow 2Al^{3+}$ substitution does not induce either an enlargement of the unit cell or a lengthening of the octahedral bond distances.

Partition of Al between Phase H and Phase D

Ohira et al. (2014) have shown that the amount of Al in the compounds belonging to the δ-AlOOH–$MgSiO_4H_2$ solid solution series increases with increasing pressure. These authors observed that perovskite and post-perovskite phases are depleted in Al_2O_3, whereas hydrous δ-AlOOH contains at least 44 mol% of $MgSiO_4H_2$ component at 68 GPa and 2010 K, and 23 mol% of this component at 128 GPa and 2190 K. Similar results were obtained by Nishi et al. (2014) who observed a strong dependence of the Al-component by pressure in Phase H. These authors noted that, although the Al contents in the starting material decrease with pressure, the Al-component in Phase H is relatively low at 40-43 GPa compared to that at about 50 GPa. Moreover, Al seems to be strongly partitioned into Phase H relative to $MgSiO_3$ perovskite and Phase D (Nishi et al. 2014).

The structural study of a grain in which both phases coexist presented here suggests that Al instead becomes strongly partitioned into Phase D relative to Phase H. As postulated by Hirose et al. (2005), at the lower mantle conditions garnet converts to Al-bearing $MgSiO_3$-perovskite, $CaSiO_3$-perovskite, and other minor phases. The Al-bearing $MgSiO_3$-perovskite in dry oceanic crust contains 15-20 mol% Al_2O_3 under these conditions (Litasov and Ohtani 2005). During the subduction of oceanic crust, a reaction between trapped water and Al-bearing $MgSiO_3$-perovskite could form Al-deficient $MgSiO_3$-perovskite and Al-rich Phase D. Then, at pressures higher than ~50 GPa, a hydrous δ-phase of the AlOOH–$MgSiO_4H_2$ solid solution (Phase H) should be stabilized. At that pressure, such a phase is able to incorporate large amount of aluminum available in hydrous peridotitic compositions in the deep lower mantle and play an important role as a water carrier in slabs descending into the lowermost mantle and core-mantle boundary.

ACKNOWLEDGMENTS

The paper benefited by the official reviews made by two anonymous reviewers. Thanks are also due to the Editor Ian Swainson for his efficient handling of the manuscript. The research was supported by "progetto di Ateneo 2013, University of Firenze" to LB, by C.N.R., Istituto di Geoscienze e Georisorse sezione di Firenze, Italy.

REFERENCES CITED

Albee, A.L., and Ray, L. (1970) Correction factors for electron probe analysis of silicate, oxides, carbonates, phosphates, and sulfates. Analytical Chemistry, 48, 1408–1414.

Bence, A.E., and Albee, A.L. (1968) Empirical correction factors for the electron microanalysis of silicate and oxides. Journal of Geology, 76, 382–403.

Bindi, L., Nishi, M., Tsuchiya, J., and Irifune, T. (2014) Crystal chemistry of dense hydrous magnesium silicates: The structure of Phase H, $MgSiH_2O_4$ synthesized at 45 GPa and 1000 °C. American Mineralogist, 99, 1802–1805.

Boffa Ballaran, T., Frost, D.J., Miyajima, N., and Heidelbach, F. (2010) The structure of a super-aluminous version of the dense hydrous-magnesium silicate phase D. American Mineralogist, 95, 1113–1116.

Frost, D.J., and Fei, Y. (1998) Stability of phase D at high pressure and high temperature. Journal of Geophysical Research, 103, 7463–7474.

Ghosh, S., and Schmidt, M.W. (2014) Melting of phase D in the lower mantle and implications for recycling and storage of H_2O in the deep mantle. Geochimica et Cosmochimica Acta, 145, 72–88.

Hirose, K., Takafuji, N., Sata, N., and Ohishi, Y. (2005) Phase transition and density of subducted MORB crust in the lower mantle. Earth and Planetary Science Letters, 237, 239–251.

Ibers, J.A., and Hamilton, W.C., Eds. (1974) *International Tables for X-ray Crystallography*, vol. IV, 366p. Kynock, Dordrecht, The Netherlands.

Komatsu, K., Sano-Furukawa, A., and Kagi, H. (2011) Effects of Mg and Si ions on the symmetry of δ-AlOOH. Physics and Chemistry of Minerals, 38, 727–733.

Litasov, K.D., and Ohtani, E. (2005) Phase relations in hydrous MORB at 18–28 GPa: implications for heterogeneity of the lower mantle. Physics of the Earth and Planetary Interiors, 150, 239–263.

Nishi, M., Irifune, T., Tsuchiya, J., Tange, Y., Nishihara, Y., Fujino, K., and Higo, Y. (2014) Stability of hydrous silicate at high pressures and water transport to the deep lower mantle. Nature Geoscience, 7, 224–227.

Ohira, I., Ohtani, E., Sakai, T., Miyahara, M., Hirao, N., Ohishi, Y., and Nishijima, M. (2014) Stability of a hydrous δ-phase, $AlOOH-MgSiO_2(OH)_2$, and a mechanism for water transport into the base of lower mantle. Earth and Planetary Science Letters, 401, 12–17.

Ohtani, E., Amaike, Y., Kamada, S., Sakamaki, T., and Hirao, N. (2014) Stability of hydrous phase H $MgSiO_4H_2$ under lower mantle conditions. Geophysical Research Letters, 41, 8283–8287.

Oxford Diffraction (2006) *CrysAlis* RED (Version 1.171.31.2) and ABSPACK in *CrysAlis* RED. Oxford Diffraction Ltd, Abingdon, Oxfordshire, England.

Pamato, M.G., Myhill, R., Boffa Ballaran, T., Frost, D.J., Heidelbach, F., and Miyajima, N. (2015) Lower-mantle water reservoir implied by the extreme stability of a hydrous aluminosilicate. Nature Geoscience, 8, 75–79.

Robinson, K., Gibbs, G.V., and Ribbe, P.H. (1971) Quadratic elongation: a quantitative measure of distortion in coordination polyhedra. Science, 172, 567–570.

Shannon, R.D. (1976) Revised effective ionic radii and systematic studies of interatomic distances in halides and chalcogenides. Acta Crystallographica, A32, 751–767.

Sheldrick, G.M. (2008) A short history of SHELX. Acta Crystallographica, A64, 112–122.

Shieh, S.R., Mao, H-K., Hemley, R.J., and Ming, L.C. (1998) Decomposition of phase D in the lower mantle and the fate of dense hydrous silicates in subducting slabs. Earth and Planetary Science Letters, 159, 13–23.

Tsuchiya, J. (2013) First principles prediction of a new high-pressure phase of dense hydrous magnesium silicates in the lower mantle. Geophysical Research Letters, 40, 4570–4573.

Yang, H., Prewitt, C.T., and Frost, D.J. (1997) Crystal structure of the dense hydrous magnesium silicate, phase D. American Mineralogist, 82, 651–654.

FIGURE CAPTIONS

FIGURE 1. Backscattered electron image of the run product synthesized at 45 GPa and 1000 °C. The different phases are labeled. White small dots are the gold derived from capsule. Scale bar is indicated.

FIGURE 2. Electron microprobe X-ray elemental maps for the crystal used for the structural study. At top left there is a backscattered electron image. The slightly shaded region above the grain is an analytical artifact due to the morphology of the crystal.

TABLE 1 – Details pertaining to the single-crystal X-ray data collections and structure refinements of Phase H and Phase D.

	Phase H	Phase D
Crystal data		
Formula	$MgSiO_4H_2$	$MgSi_2O_6H_2$
Crystal system	orthorhombic	trigonal
Space group	*Pnnm*	$P\bar{3}1m$
a (Å)	4.730(2)	4.752(2)
b (Å)	4.324(2)	4.752(2)
c (Å)	2.843(2)	4.314(2)
V (Å^3)	58.15(5)	84.37(6)
Z	1	1
Data collection		
Instrument	Oxford Diffraction Xcalibur 3	
Radiation type	Mo$K\alpha$ (λ = 0.71073 Å)	
Temperature (K)	293(2)	
Det. to sample dist. (cm)	6	
Number of frames	285	312
Measuring time (s)	200	
Maximum covered 2θ (°)	52.86	49.78
Absorption correction	multi-scan (*ABSPACK*; Oxford Diffraction 2006)	
Collected reflections	504	590
Unique reflections	73	64
Reflections with $F_o > 4\sigma(F_o)$	37	35
R_{int}	0.0318	0.0360
R_σ	0.0421	0.0451
Range of h, k, l	$-5 \le h \le 5$, $-5 \le k \le 5$, $-3 \le l \le 3$	$-5 \le h \le 5$, $-5 \le k \le 5$, $-5 \le l \le 5$
Refinement		
Refinement	Full-matrix least squares on F^2	
Final R_1 [$F_o > 4\sigma(F_o)$]	0.0240	0.0203
Final R_1 (all data)	0.0250	0.0262
No. ref. parameters	6	7
$\Delta\rho_{max}$ (e Å^{-3})	0.47	0.24
$\Delta\rho_{min}$ (e Å^{-3})	-0.59	-0.29

TABLE 2. Fractional atomic coordinates, site-occupancy factors (s.o.f.) derived from electron microprobe, isotropic displacement parameters (Å^2) and geometric parameters (Å, Å^3, º) for Phase H and Phase D.

Phase H					
	s.o.f.	*x*	*y*	*z*	U_{iso}
M	$Mg_{0.500}Si_{0.465}Al_{0.035}$	0	0	0	0.018(5)
O	$O_{1.00}$	0.3481(6)	0.2297(9)	0	0.017(1)
M-O (×2)	1.923(3)				
M-O (×4)	1.975(3)				
<M-O>	1.958				
σ^2	1.58				
V	10.00				
Phase D					
	s.o.f.	*x*	*y*	*z*	U_{iso}
Mg	$Mg_{1.00}$	0	0	0	0.027(1)
M	$Si_{0.75}Al_{0.25}$	1/3	2/3	1/2	0.0204(5)
O	$O_{1.00}$	0.6462(4)	0	0.2740(4)	0.027(1)
Mg-O (×6)	2.055(2)	M-O (×6)	1.821(2)		
σ^2	0.05	σ^2	25.25		
V	11.57	*V*	7.96		

* Angle variance (σ^2) calculated according to Robinson et al. (1971).

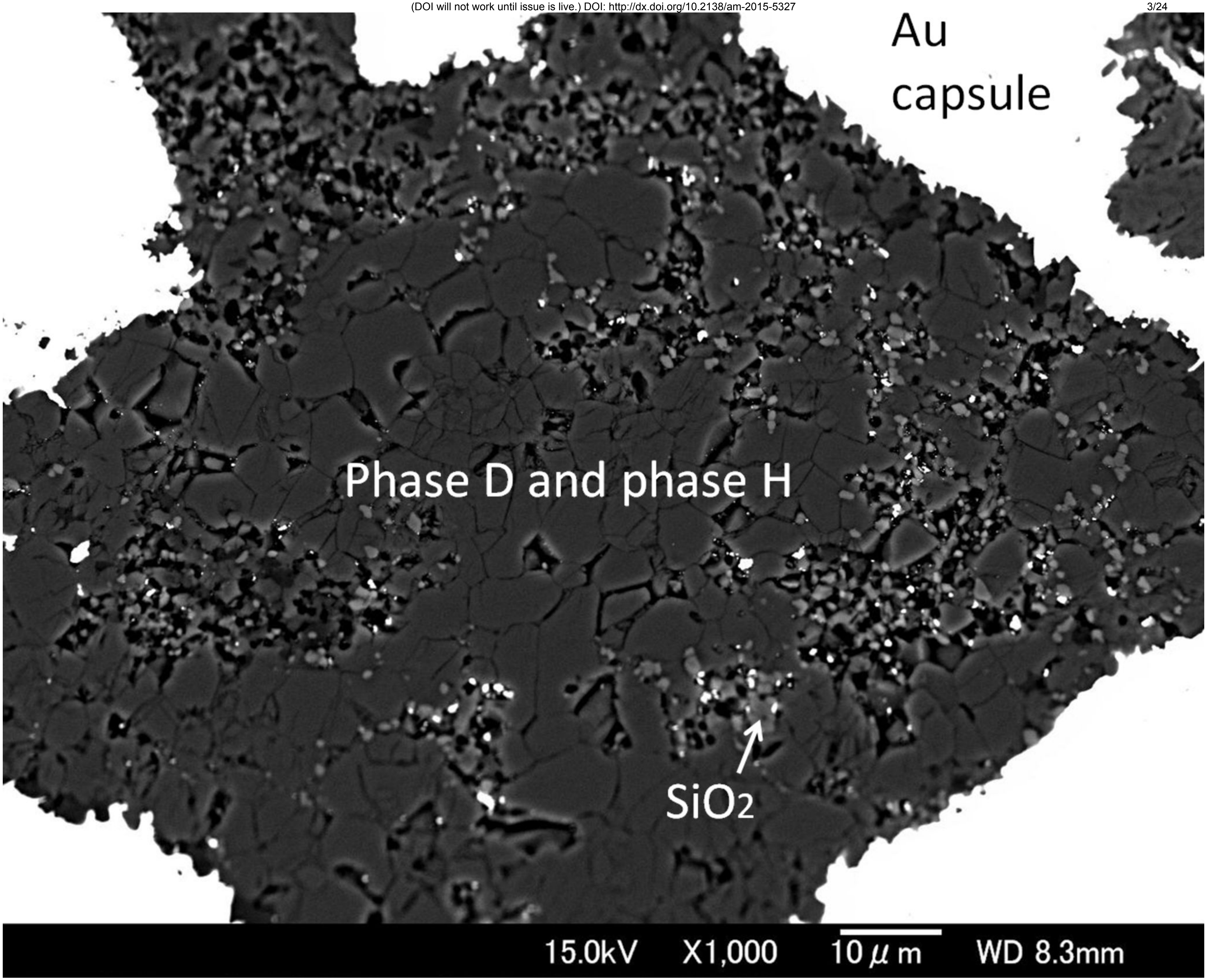
Au capsule
Phase D and phase H
SiO2
15.0kV
X1,000
10 μm
WD 8.3mm

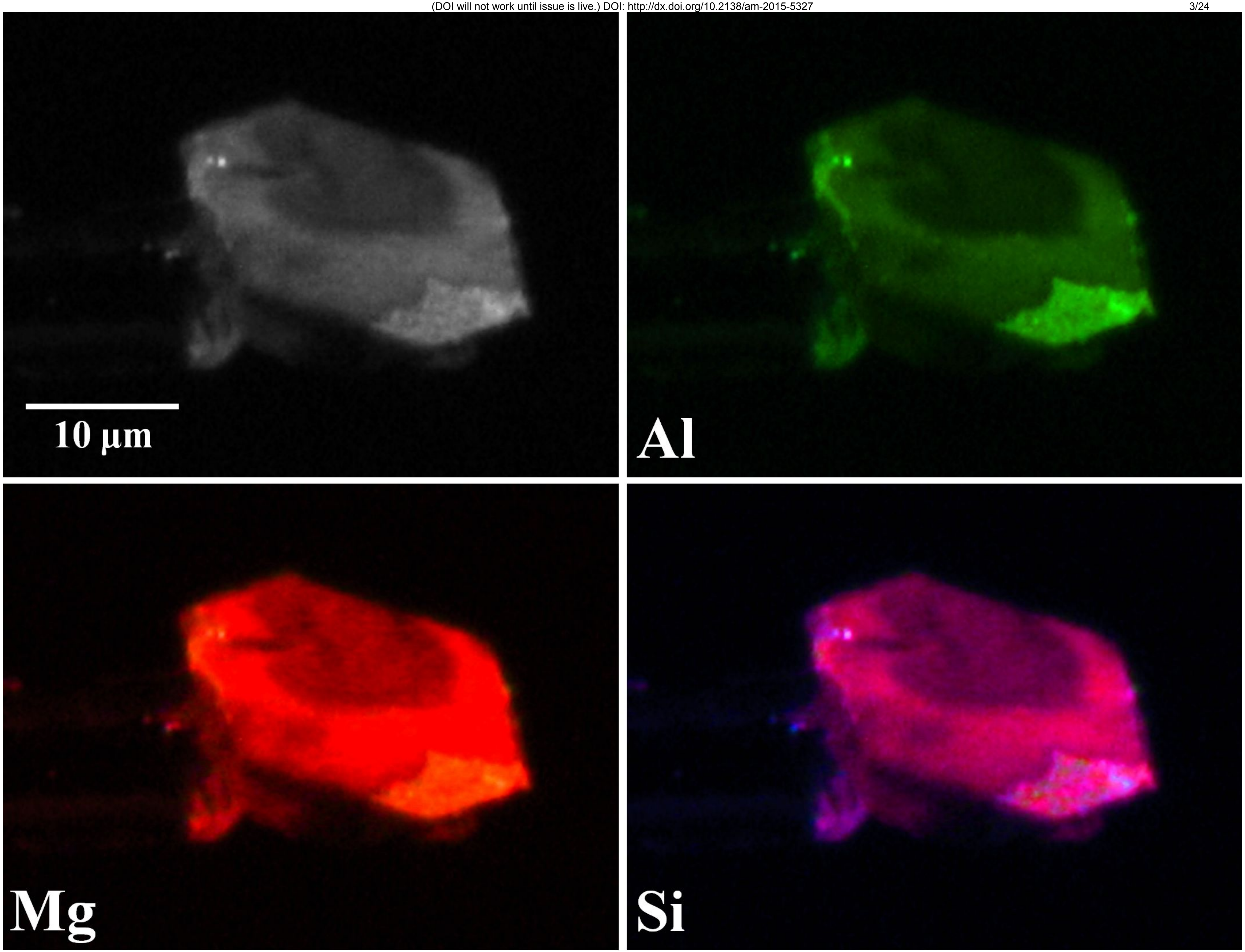
10 µm
Al
Mg
Si